

# Pre-seismic ionospheric anomalies detected before the 2016 Taiwan earthquake

Shin-iti Goto<sup>1</sup>, Ryoma Uchida<sup>1</sup>, Kiyoshi Igarashi<sup>1</sup>, Chia-Hung Chen<sup>2</sup>, and Ken Umeno<sup>1\*</sup>

<sup>1</sup> Department of Applied Mathematics and Physics,

Graduate School of Informatics, Kyoto University, Kyoto, Japan.

<sup>2</sup> Department of Earth Sciences, National Cheng Kung University, Tainan, Taiwan.

December 22, 2022

## Abstract

On Feb. 5 2016 (UTC), an earthquake with moment magnitude 6.4 occurred in southern Taiwan, known as the 2016 (Southern) Taiwan earthquake. In this study, evidences of seismic earthquake precursors for this earthquake event are investigated. Results show that ionospheric anomalies in Total Electric Content (TEC) can be observed before the earthquake. These anomalies are obtained by processing TEC data, where such TEC data are calculated from phase delays of signals observed at densely arranged ground-based stations in Taiwan for Global Navigation Satellite Systems. In this paper, it is shown how pre-seismic activity caused by this earthquake can be observed in terms of TEC in the ionosphere, and that one such anomalies were detected within one hour before the event.

## keypoints:

Precursors to the 2016 Taiwan earthquake is found in the ionosphere in analyzing TEC data.

## 1 Introduction

The ionosphere is an ionized medium which can affect the radio communications. The electron density in the ionosphere is disturbed by various phenomena such as solar flares[*Donnelly(1976)*], volcanic eruptions[*Igarashi et al.(1994)*], flying objects[*Mendillo et al.(1975)*], earthquakes[*Ogawa et al.(2012)*], and so on. These electron density disturbances are observed with Total Electron Contents (TECs) at ground-based Global Navigation Satellite Systems (GNSS) receivers. With GNSS that can monitor variations of TEC, it has been reported [*Heki(2011)*, *Heki and Enomoto(2015)*] that pre-seismic ionospheric electron density anomalies appeared frequently before large earthquakes, which could be caused by the earthquake-induced electromagnetic process before such earthquakes. Furthermore, such TEC anomalies were found in the 2016 Kuramoto earthquake (Mw7.3) [*Iwata and Umeno(2017)*].

Taiwan is located in an active seismic area [*Liu et al(2000)*, *Oyama et al.(2008)*] and has ground-based stations for GNSS with densely arranged receivers. Thus, Taiwan is a suitable region to explore a relation between an earthquake and pre-seismic ionospheric TEC anomalies. An earthquake occurred around southern Taiwan in Feb. 2016 (19:57 UTC, 5 Feb. 2016, Mw6.4, depth 23.0 km, 22.94 N 120.6 E ). As reported in U.S. Geological Survey [*USGS(2016)*], this event was the result of oblique thrust faulting at shallow-mid crustal depths. Rupture occurred on a fault oriented either northwest-southwest, and dipping shallowly to the northeast, or on a north-south striking structure dipping steeply to the west. At the location of the earthquake, two tectonic plates converge in a northwest-southeast direction at a velocity of about 80 mm a year.

In this paper pre-seismic ionospheric TEC anomalies for the 2016 Taiwan earthquake (Mw 6.4) are shown with the method described in [*Iwata and Umeno(2016)*]. With this method, the TEC anomalies

---

\*umeno.ken.8z@kyoto-u.ac.jp

were detected for the Kuramoto earthquake [Iwata and Umeno(2017)], where this earthquake is classified as an intraplate earthquake and its momentum magnitude is less than 8. It is then of interest to explore if TEC anomaly is observed with this method for intraplate earthquakes whose momentum magnitudes are less than 7.

## 2 Method

The TEC along the line of sight, called slant TEC, can be calculated with the phase delay of signals sent from GNSS satellites observed at ground-based GNSS receivers. In the following slant TEC is abbreviated as TEC, and TEC data were calculated from signals sent from the Global Positioning System (GPS, American GNSS) satellites. Also, the standard unit, TECU that is  $10^{16}[\text{ele}/\text{m}^2]$ , is used. For simplifying various calculations, electrons in the ionosphere are approximated to be in a thin layer, and this layer for Taiwanese GNSS stations is set to 325 km from the ground. At this height, the electron density is the maximum in the ionosphere. The intersection of the line of sight from a GNSS station with this thin layer is called ionospheric piercing point, and its projection onto the surface of the earth is called Sub-Ionospheric Point (SIP). SIP tracks shown in this paper were calculated with the height of the thin layer.

For large earthquakes various techniques using TEC data can detect earthquake precursors. One of those is the correlation method [Iwata and Umeno(2016)]. This method is summarized as follows.

1. Choose a central GNSS station, a satellite, and three parameters denoted by  $t_{\text{sample}}$ ,  $t_{\text{test}}$ , and  $M$ . The parameter  $t_{\text{sample}}$  is the time-length of data used for obtaining a regression curve,  $t_{\text{test}}$  the time-length for testing the difference between the regression curve and the obtained data, and  $M$  the number of GNSS stations located around the central station for the correlation analysis. Here and in what follows the time unit is taken to be one hour. We fix  $t_{\text{sample}}$  and  $t_{\text{test}}$  to be 2 and 0.25 throughout this paper.
2. Let SampleData be the TEC data for the time-duration from  $t$  to  $t+t_{\text{sample}}$  for each station labeled by  $i$ . Also, let TestData be the TEC data for the time-duration from  $t+t_{\text{sample}}$  to  $t+t_{\text{sample}}+t_{\text{test}}$ .
3. Fit a curve to SampleData by the least square method with a polynomial curve whose degrees is seven.
4. Calculate a deviation of TestData from the regression curve for the time-duration  $t_{\text{test}}$ , and such a deviation is denoted by  $x_{i,t'}$  where  $t'$  is such that  $t_{\text{sample}} \leq t' \leq t_{\text{sample}} + t_{\text{test}}$ .
5. Calculate the correlation defined as

$$C(T) = \frac{1}{NM} \sum_{i=1}^M \sum_{j=0}^{N-1} x_{i,t+t_{\text{sample}}+j\Delta t} x_{0,t+t_{\text{sample}}+j\Delta t},$$

where  $T = t+t_{\text{sample}}+t_{\text{test}}$ ,  $N$  is the number of data points for TestData,  $\Delta t$  the sampling interval for TestData so that  $\Delta t = t_{\text{test}}/(N-1)$ , and  $i=0$  the special label indicating the central GNSS station.

In what follows the word ‘‘anomaly’’ is used, when the correlation value is large enough. To quantify and define abnormality, careful discussions are needed. Any definition of abnormality is not given in this paper, however, we compare correlation values in view of days and distances among GNSS stations. The details of these are discussed in Section 3.

## 3 Data Presentation

In this section the results of the correlation analysis method applied to the earthquake are shown. TEC data were obtained from the original GPS data with the method in [Otsuka et al.(2002)], and the original GPS data were obtained from the Central Weather Bureau (CWB) in Taiwan (R.O.C.).

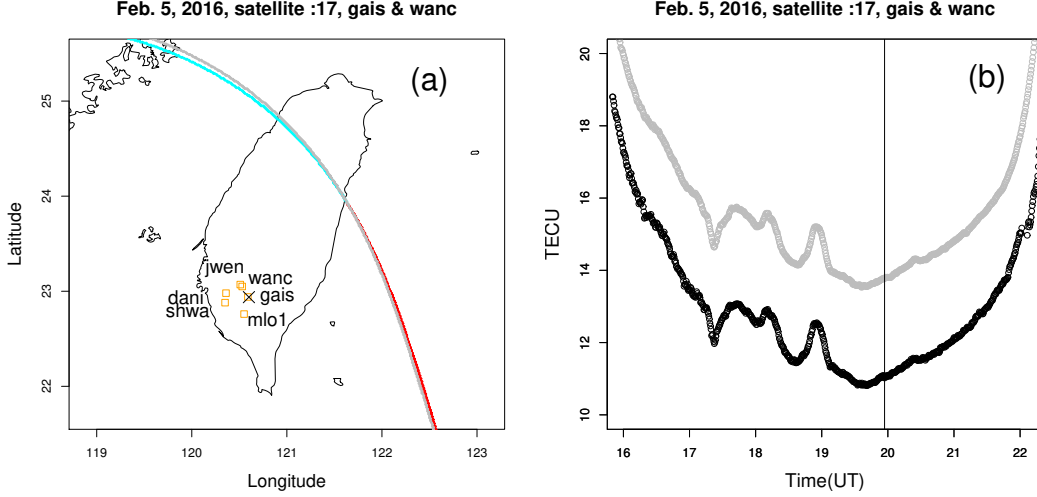


Figure 1: (a) SIP tracks of GPS satellite 17 on Feb. 5 in 2016, and various GNSS stations. Red curve: SIP track observed at “gais” after the event, Cyan curve: SIP track observed at “gais” before the event, Gray curve: SIP track observed at “wanc”,  $\times$  : Epicenter, Orange  $\square$  : Stations for calculating correlations with  $M = 5$ . (b) TEC changes as time-series associated with GPS satellite 17 observed at “gais” (black) and at “wanc” (gray), where the TEC values obtained at “wanc” were shifted by hand for the guide of eyes. The vertical line indicates the time (UT) when the event occurred.

Figure 1 (a) shows SIP tracks of GPS satellite 17 associated with the stations “gais” and “wanc”. Figure 1 (b) shows TEC changes as time-series observed at “gais” and “wanc”. These figures contain the basic information regarding the discussions below.

Figure 2 shows the time-series of TEC data observed for the consecutive 9 days including the day when the event occurred. These time-series were obtained with GPS satellite 17 associated with the stations “gais” and “wanc”. From this figure, it is verified that the obtained 2 time-series on each day are similar to each other. It is reasonable, since these 2 stations are geographically close. Time-series of correlations shown below were obtained by processing this kind of TEC data.

Figure 3 shows the time-series of correlations with  $M = 1$  for the consecutive 9 days including the day when the event occurred. The number of the GNSS stations which we employ is kept to 2. The central GNSS station is chosen to be “gais”, since it is the nearest station from the epicenter. The distance between them is about 1.0 km. The other station is “wanc”, and it is the next nearest station for which TEC data is available. The distance between “wanc” and the epicenter is about 14.1 km. As it can be read off, about 40 min. before the event, a period of time was observed where correlation values are large. Its maximum value is 128, which was observed at 19:23. Whereas there are some periods where correlation values are large on Jan. 28 and Feb. 1. Their characteristics of time-series are different to that on Feb. 5. Such anomalous periods on Jan. 28 and Feb. 1 are situated around the times when time-series start. In addition the largest value of the correlation on Jan. 28 is about half of that on Feb. 5. Besides, the largest value of the correlation on Feb. 1 is 1/3 of that on Feb. 5.

Figure 4 shows the time-series of correlations with  $M = 5$  for the consecutive 9 days including the day when the event occurred. The central station is “gais” that is the nearest one from the epicenter. The other stations are chosen as “wanc”, “jwen”, “mlo1”, “dani”, and “shwa” so that they are located near the epicenter. When the number of stations for the correlation analysis increases, it is expected that the correlation values become larger than that of the case with  $M = 1$ , if each station receives common sudden disturbed signals. On the day when the event occurred, the obtained time-series is consistent with the case with  $M = 1$  presented above. For the days Feb. 1 and Jan. 28, on which correlation values are large but no event, the maximum values decrease by more than half of those for the case with  $M = 1$ . Combining these, we see that the anomaly in time-series on Feb. 5 appeared commonly around the central station “gais”. On the contrary, anomalies on Feb. 1 and Jan. 28 did not appear commonly around “gais”.

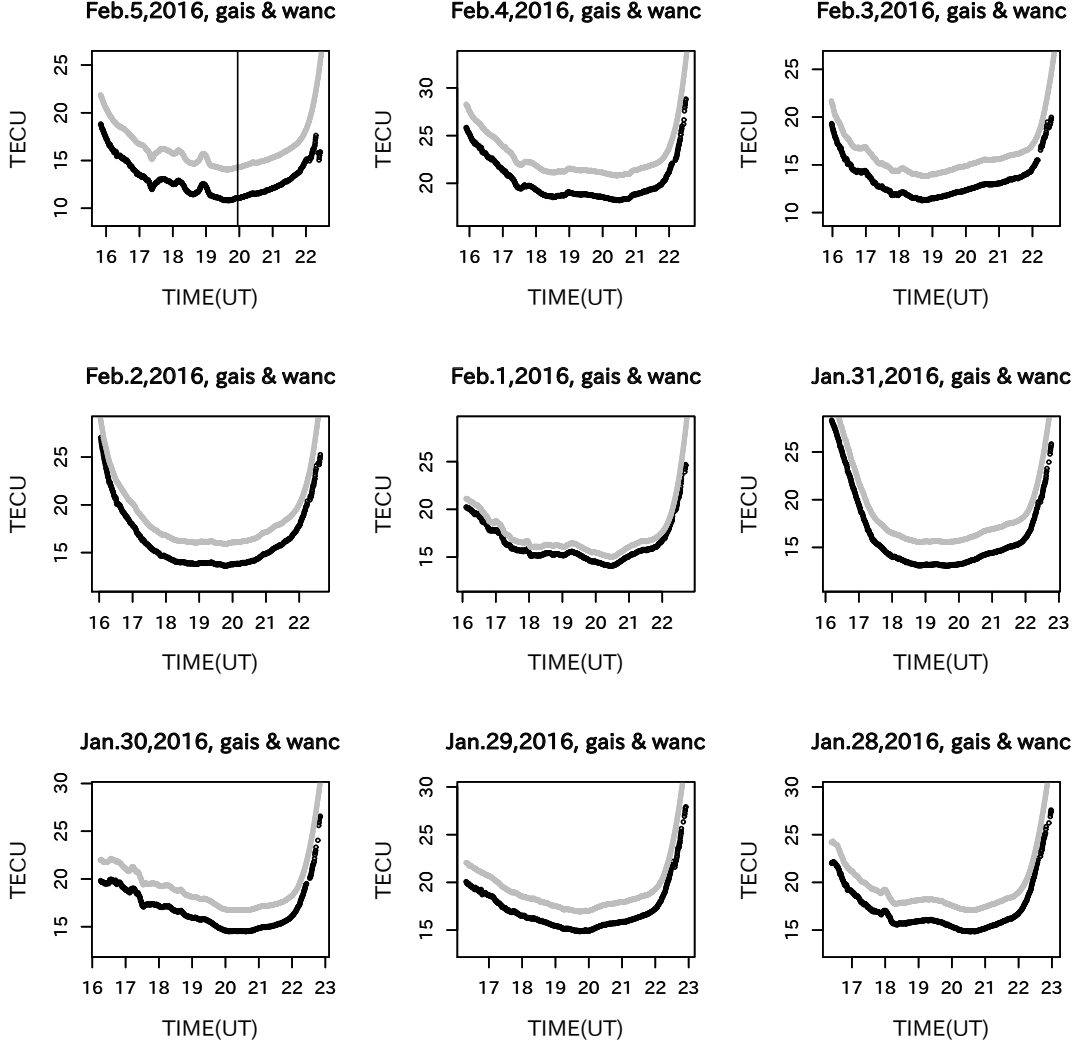


Figure 2: Time-series of TEC data observed at the stations “gais” (black) and “wanc” (gray) for the period from Jan. 28 to Feb. 5 in 2016, where the TEC values obtained at “wanc” were shifted by hand for the guide of eyes. GPS satellite 17 was used, and the vertical line on Feb. 5 indicates the time when the event occurred.

Figure 5 shows time-series of correlations with  $M = 1$  for the period from Jan. 18 to Jan. 27 in 2016, except for Jan. 24th. On Jan. 24, no data were acquired. No significant anomaly was observed in this period, and this observation is consistent with the non-existence of significant geomagnetic activity ( see Section 4 ).

## 4 Discussion

In Section 3, TEC anomalies before the earthquake have been shown. To give another evidence that such TEC anomalies were caused by the Taiwan earthquake, our correlation analysis can also be applied to time-series of TEC data obtained in Japan on the same day. GNSS data were obtained from the Geospatial Information Authority of Japan. The distance between Taipei and Fukuoka located the south part of Japan is about 1280 km, and the correlation analysis applied to TEC data observed in Japan provides how much Medium-Scale Traveling Ionospheric Disturbance (MSTID) occurred, where Japan is located upstream of MSTID [Hunsucker(1982), Otsuka et al.(2011)]. Here MSTID is known as

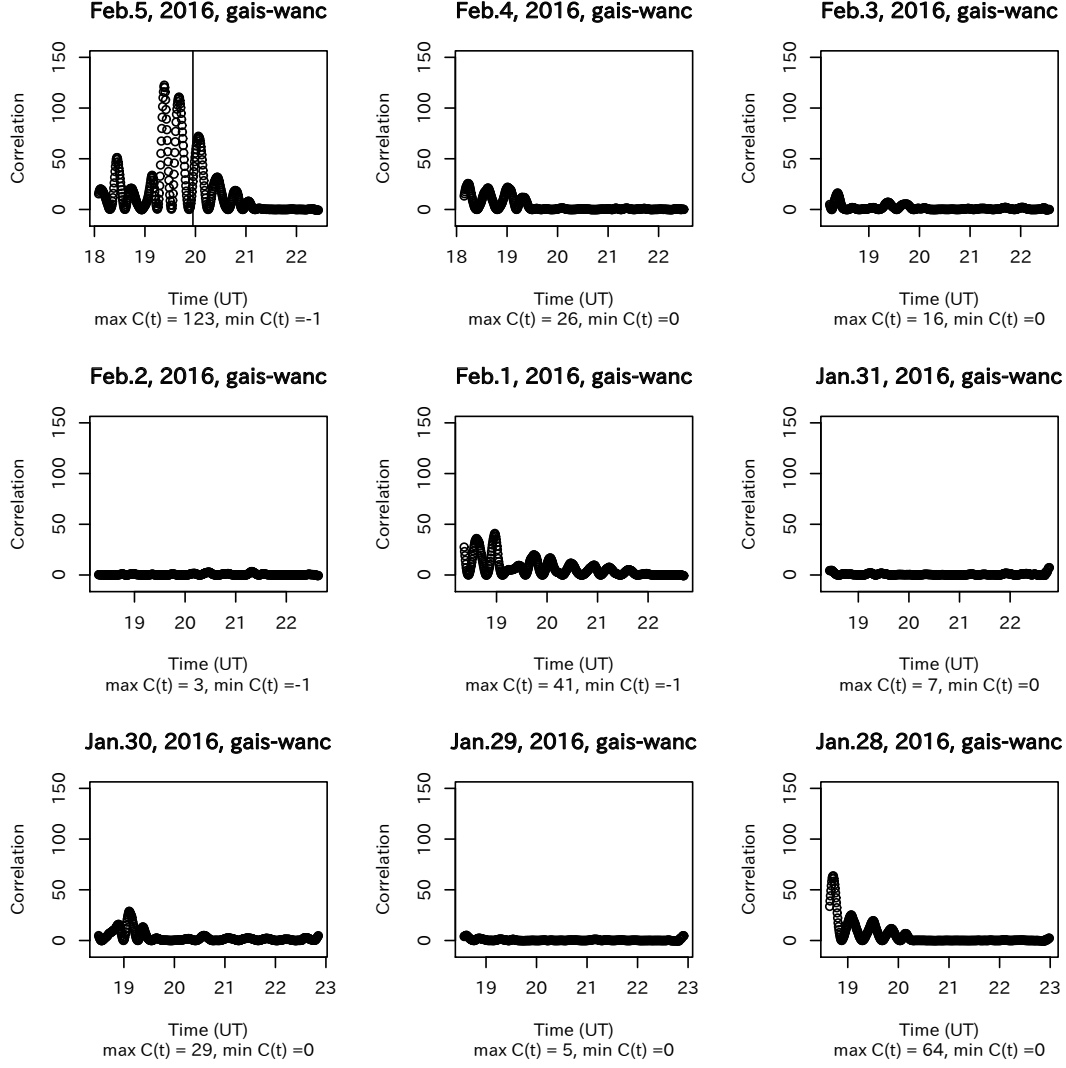


Figure 3: Time-series of correlations  $M = 1$  obtained with TEC data observed at the stations "gais" and "wanc" for the period from Jan. 28 to Feb. 5 in 2016. GPS satellite 17 was used. The vertical line on Feb. 5 indicates the time when the event occurred.

a type of disturbance in the ionosphere, and it might hide TEC anomalies as an earthquake precursor.

Figure 6(a) shows the time-series of correlations with  $M = 30$  obtained with TEC data observed at various GNSS stations in Japan 30 min. before the event, where TEC data were calculated with GPS satellite 28. It suggests that there was no significant TEC anomaly and MSTID around Japan. Here Japan is located upstream of MSTID for Taiwan. Figure 6(b) shows SIP track observed at GNSS station "0087", Fukuoka in Japan. For the both of figures, GPS satellite 28 was used, and the ionosphere is assumed to be a thin layer located at 300 km from the ground. From these data concerning the upstream of MSTID, there was no disturbance due to MSTID around the time when the anomalies in Taiwan were observed.

Geomagnetic variations indices of  $K_p$  and  $Dst$  are examined during 2 weeks from Jan. 23 to Feb. 5, 2016 on this earthquake day and earlier. Provisional  $Dst$  indices show variations between  $-53$  and  $17$  during this period. No Sudden Storm Commencement was observed during this period, and then this period was under relatively quiet geomagnetic conditions. Therefore it is presumed that the analyzed

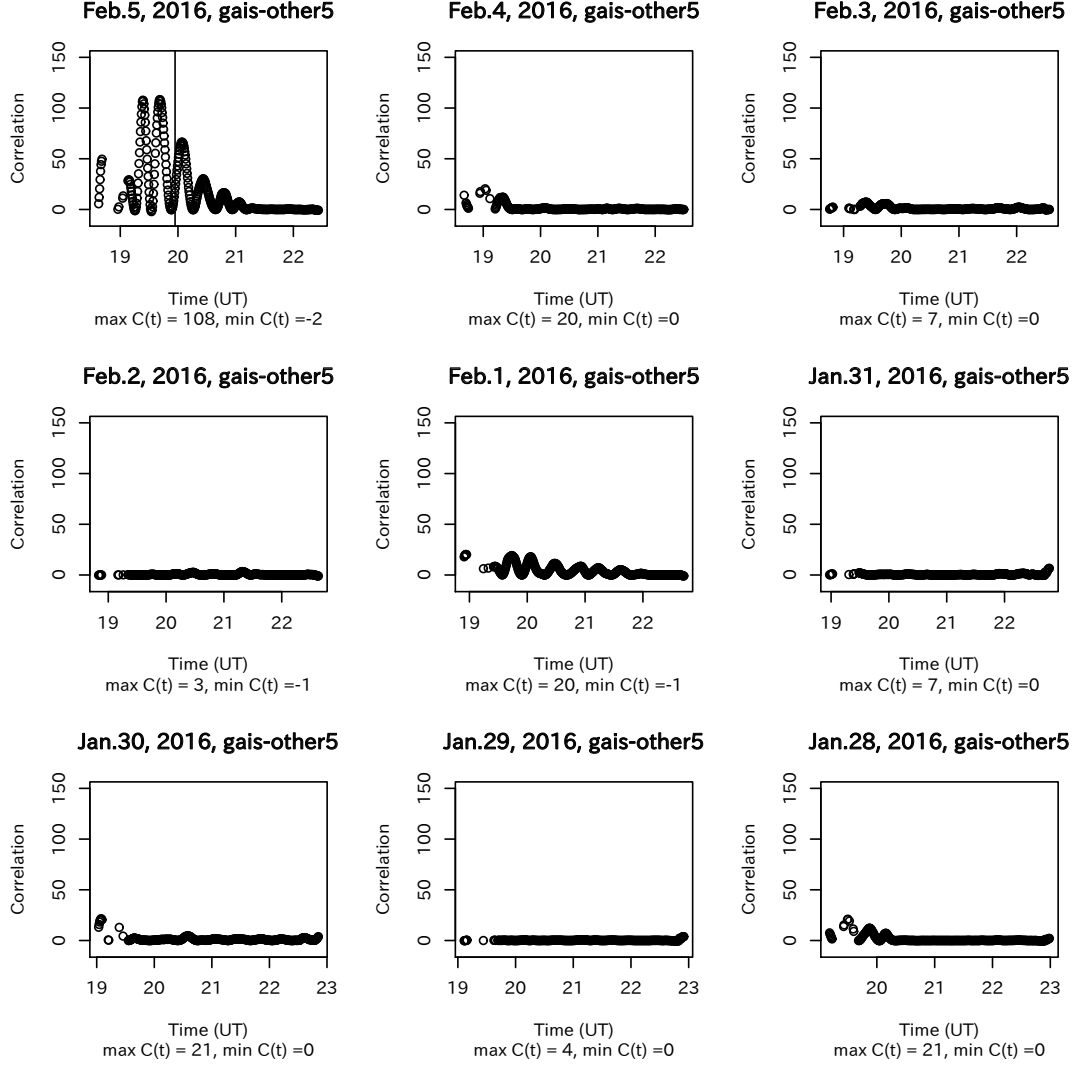


Figure 4: Time-series of correlations with  $M = 5$  obtained with TEC data observed at 6 stations for the period from Jan. 28 to Feb. 5 in 2016. GPS satellite 17 was used, and the central station is “gais”, and the other 5 stations are “wanc”, “jwen”, “mlo1”, “dani”, “shwa”. The vertical line on Feb. 5 indicates the time when the event occurred.

period of TEC variations are not contaminated by relatively large geomagnetic disturbances.

To explain TEC anomalies responsible for large earthquakes, several models consisting of electromagnetic processes due to stressed rocks have been proposed. Recent progress of such has been summarized in [He and Heki(2017)]. Such models are Lithosphere-atmosphere-ionosphere (LAI) coupling models, and one of them is based on the experimental results on stressed rocks [Freund(2013)]. In [Heki and Enomoto(2015)], differences between intraplate earthquakes and interplate ones with  $M_w \geq 8.2$  were argued, and then each mechanism that causes precursors could be different each other. Since the focus of this study is an intraplate earthquake with  $M_w 6.4$ , the existing models for observed TEC anomalies may not be suitable. To clarify a physical mechanism of the TEC anomalies, further investigations are needed.

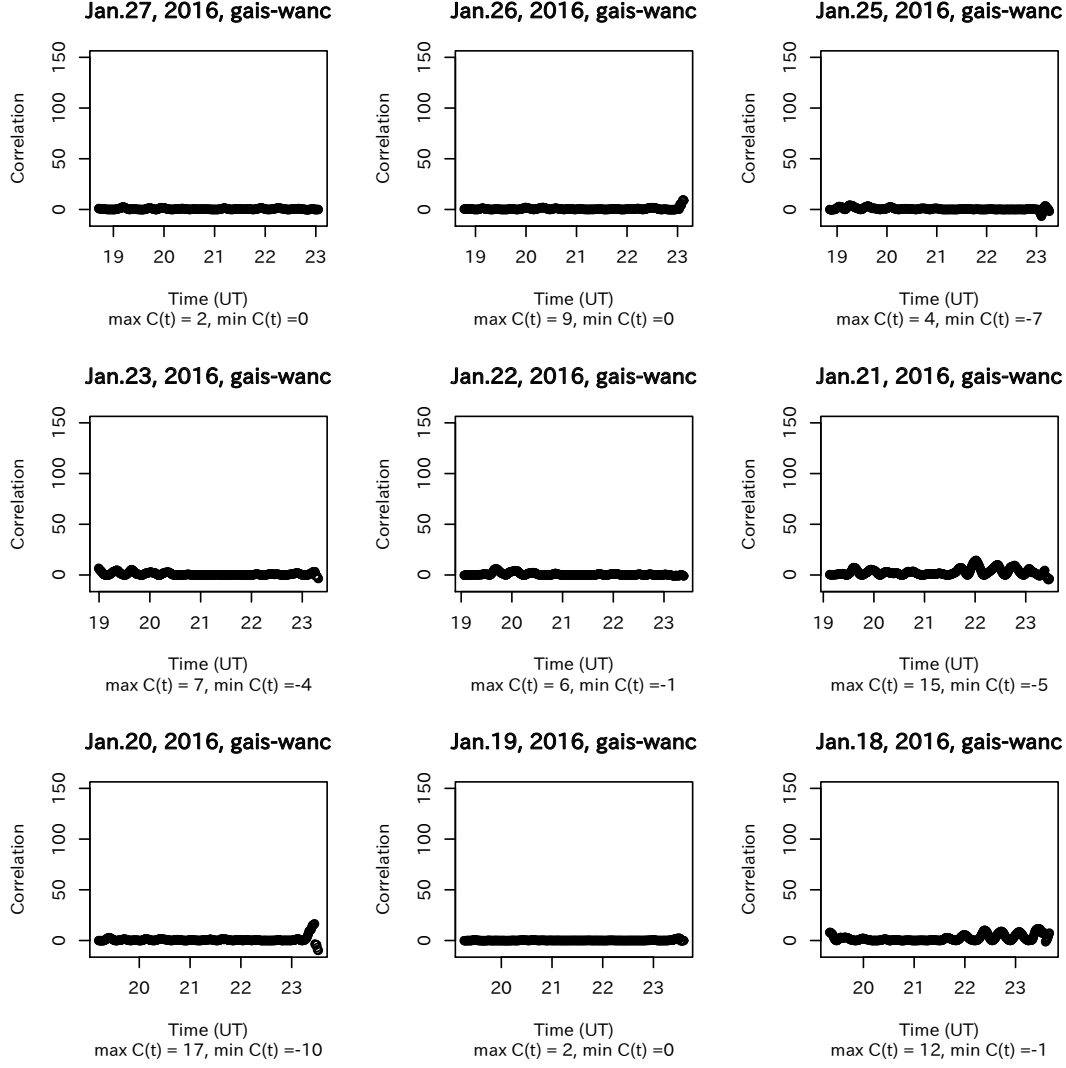


Figure 5: Time-series of correlations with  $M = 1$  obtained with TEC data observed at the stations “gais” and “wanc” for the period from Jan. 18 to Jan. 27 in 2016, except for Jan. 24.

## 5 Conclusions

It has been shown how a TEC anomaly can be detected prior to the 2016 Taiwan earthquake. This earthquake is with Mw 6.4, and is classified as a type of intraplate one. With the correlation analysis, the TEC anomalies have been detected about 40 min. before the event. Since it had not been known such an hour-long earthquake precursor for this class of moment magnitudes, this finding is a first example for showing such a precursor. One candidate of the reasons why this anomaly can appear is that the 2016 Taiwan earthquake is intraplate one. There are some future works involving this study. One is to explore why this anomaly in the ionosphere appears with models such as the LAI coupling model. Another one is to apply this correlation analysis to some intraplate earthquakes. The later is expected to reveal conditions when this type of anomaly in the ionosphere is observed.

## Acknowledgments

The authors thank Dr. T. Yoshiki for fruitful discussions, the Geospatial Information Authority of Japan (GSI) for providing the GPS data in Japan, the Central Weather Bureau in Taiwan for providing the GPS

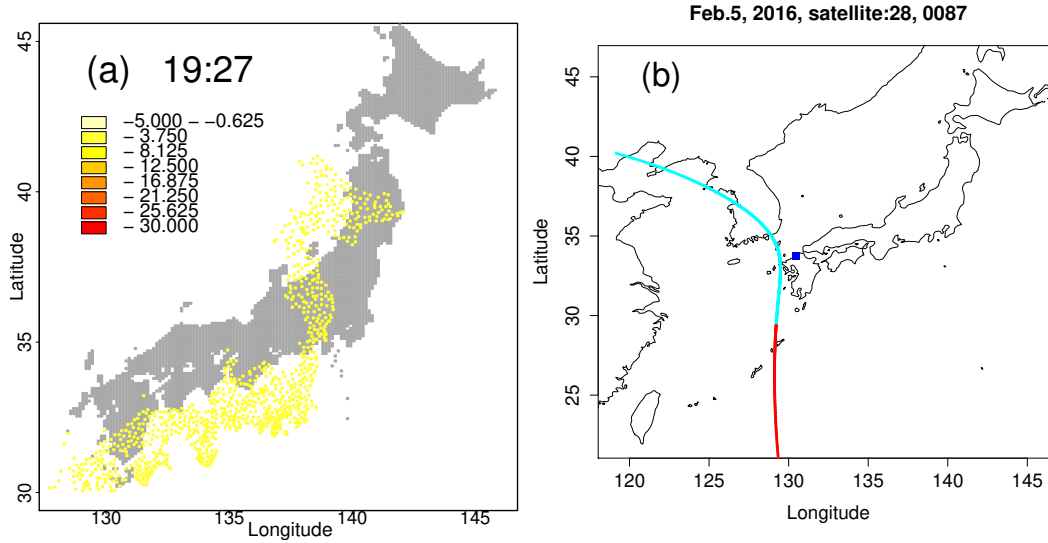


Figure 6: (a) Time-series of correlations with  $M = 30$  obtained with TEC data observed at various stations in Japan at 19:27(UT) on Feb. 5, 2016. Here GPS satellite 28 was used. (b) SIP track observed at 0087(“Koga” in Fukuoka, blue) associated with GPS satellite 28. Cyan curve: before the event, and Red curve: after the event.

data in Taiwan. Also, the authors belonging to Kyoto university acknowledge K-Opticom cooperation for continuous support regarding the Kyoto University-K-Opticom collaborative research agreement (2017-2020). C. H. Chen is supported by Central Weather Bureau (CWB) of Taiwan (R.O.C.) to National Cheng Kung University under MOTC-CWB-107-E-01. The GPS observations were provided by the Central Weather Bureau (CWB) of Taiwan (R.O.C.).

## References

- [Donnelly(1976)] Donnelly, R.F. (1976), Empirical models of solar flare X-ray and EUV emission for use in studying their E and F region effects, *J. Geophys. Res.*, 81, 4745–4753.
- [Freund(2013)] Freund, F. (2013), Earthquake forewarning – A multidisciplinary challenge from the ground up to space, *Acta Geophys.*, 61, 775–807, doi:10.2478/s11600-009-0066-x.
- [He and Heki(2017)] He, L., and K. Heki (2017), Ionospheric anomalies immediately before Mw7.0-8.0 earthquakes, *J. Geophys. Res. Space Physics.*, 122, doi:10.1002/2017JA024012.
- [Heki(2011)] Heki, K. (2011), Ionospheric electron enhancement preceding the 2011 Tohoku-Oki earthquake, *J. Geophys. Res. Lett.*, 38, L17312, doi:10.1029/2011GL047908.
- [Heki and Enomoto(2015)] Heki, K., and Y. Enomoto (2015), Mw dependence of the preseismic ionospheric electron enhancements, *J. Geophys. Res. Space Physics*, 120, 70006-7020, doi:10.1002/2015JA021353.
- [Hunsucker(1982)] Hunsucker, R (1982), Atmospheric gravity waves generated in the high latitude ionosphere: a review, *Rev. Geophys.*, 20, 293–315.
- [Igarashi et al.(1994)] Igarashi, K., S. Kainuma, I. Nishimuta, S. Okamoto, H. Kuroiwa, T. Tanaka, and T. Ogawa (1994), Ionospheric and atmospheric disturbances around Japan caused by the eruption of Mount Pinatubo on 15 June 1991, *J. Atmos. Terr. Phys.*, 56, 1227–1234.
- [Iwata and Umeno(2016)] Iwata, T., and K. Umeno (2016), Correlation analysis for preseismic total electron content anomalies around the 2011 Tohoku-Oki earthquake, *J. Geophys. Res. Space Physics*, 121, 8969-8984, doi:10.1002/2016JA023036.



- [*Iwata and Umeno(2017)*] Iwata, T., and K. Umeno (2017), Preseismic ionospheric anomalies detected before the 2016 Kumamoto earthquake, *J. Geophys. Res. Space Physics.*, 122, 3602-3616, doi:10.1002/2017JA023921.
- [*Kelly et al.(2017)*] Kelly, M.C., W.E. Swartz, and K. Heki (2017). Apparent ionospheric total electron content variations prior to major earthquakes due to electric fields created by tectonic stresses. *J. Geophys. Res. Space Physics.*, 122, doi:10.1002/2016JA023601.
- [*Liu et al.(2000)*] Liu, J.Y., T.I. Chen, S.A. Pulnits, Y.B. Tsai, and Y.J. Chuo, (2000), Seismo-ionospheric signatures prior to  $M \geq 6.0$  Taiwan earthquakes, *Geophysical Research Letters*, 27, 3113–3116.
- [*Mendillo et al.(1975)*] Mendillo, M., G.S. Hawkins, and J.A. Klobuchar (1975), A sudden vanishing of the ionospheric F region due to the launch of Skylab, *J. Geophys. Res.*, 80, 2217–2225,
- [*Ogawa et al.(2012)*] Ogawa, T., N. Nishitani, T. Tsugawa, and K. Shiokawa (2012), Giant ionospheric disturbance observed with the SuperDARN Hokkaido HF radar and GPS network after the 2011 Tohoku earthquake. *Earth Planet Space*, 64, 1295–1307.
- [*Otsuka et al.(2011)*] Otsuka, Y., N. Kotake, K. Shiokawa, T. Ogawa, T. Tsugawa, and A Saito (2011), Statistical study of medium-scale traveling ionospheric disturbances observed with a GPS receiver network in Japan, in Aeronomy of the Earths Atmosphere and Ionosphere, *IAGA Spec. Sopron Book Ser.*, vol. 2, pp. 291299, Springer, Netherlands, doi:10.1007978-94-007-0326-1\_21.
- [*Otsuka et al.(2002)*] Otsuka, Y., T. Ogawa, A. Saito, T. Tsugawa, S. Fukao, and S. Miyazaki, A(2002), New technique for mapping of total electron content using GPS network in Japan, *Earth Planet Space*, 54, 63–70.
- [*Oyama et al.(2008)*] Oyama, K.-I., K. Kakinami, J.Y. Liu, M. Kamogawa, and T. Kodama (2008), Reduction of electron temperature in low-latitude ionosphere at 600 km before and after large earthquakes. *J. Geophys. Res.*, 113, A11317.
- [*USGS(2016)*] USGS Report,  
<https://earthquake.usgs.gov/earthquakes/eventpage/us20004y6h#executive>